JOURNAL OF GEOPHYSICAL RESEARCH, VOL. 98, NO. A11, PAGES 19,223–19,234, NOVEMBER 1, 1993

Effects of a Parallel Electric Field and the Geomagnetic Field in the Topside Ionosphere on Auroral and Photoelectron Energy Distributions

Q.-L. MIN, D. LUMMERZHEIM, M. H. REES, AND K. STAMNES

Geophysical Institute and Physics Department, University of Alaska, Fairbanks

The consequences of electric field acceleration and an inhomogeneous magnetic field on auroral electron energy distributions in the topside ionosphere are investigated. The one-dimensional, steady state electron transport equation includes elastic and inelastic collisions, an inhomogeneous magnetic field, and a field-aligned electric field. The case of a self-consistent polarization electric field is considered first. The self-consistent field is derived by solving the continuity equation for all ions of importance, including diffusion of O^+ and H^+, and the electron and ion energy equations to derive the electron and ion temperatures. The system of coupled electron transport, continuity, and energy equations is solved numerically. Recognizing observations of parallel electric fields of larger magnitude than the baseline case of the polarization field, the effect of two model fields on the electron distribution function is investigated. In one case the field is increased from the polarization field magnitude at 300 km to a maximum at the upper boundary of 800 km, and in another case a uniform field is added to the polarization field. Substantial perturbations of the low energy portion of the electron flux are produced: an upward directed electric field accelerates the downward directed flux of low-energy secondary electrons and decelerates the upward directed component. Above about 400 km the inhomogeneous magnetic field produces anisotropies in the angular distribution of the electron flux. The effects of the perturbed energy distributions on auroral spectral emission features are noted.

INTRODUCTION

Numerous studies during the past quarter century have shown that auroral electron precipitation into the Earth's atmosphere produces substantial enhancements or perturbations in several ionospheric and atmospheric parameters such as ionization, excitation, and thermal effects. These studies, however, have not considered the possibility that aurorally produced changes in atmospheric/ionospheric parameters may, in turn, cause perturbations to the phase space distribution of the precipitating electrons. This possibility could not be investigated quantitatively prior to the development of electron transport codes that compute the evolution of the electron intensity $I(z, \epsilon, \mu)$ as a function of altitude z, energy ϵ, and pitch angle μ as the stream penetrates into the inhomogeneous atmosphere. Electron transport has been studied by several investigators in recent years [*Berger et al.*, 1970; *Banks and Nagy*, 1970; *Nagy and Banks*, 1970; *Mantas*, 1975; *Strickland et al.*, 1976; *Jasperse*, 1977; *Stamnes*, 1980; *Stamnes*, 1981; *Porter et al.*, 1987; *Lummerzheim*, 1987; *Lilensten*, 1989; *Link*, 1992]. All investigators start either with an embedded photoelectron source and/or with a flux at the upper boundary representing conjugate photoelectrons and/or auroral electrons. The energetic electrons are allowed to be scattered and degraded in energy by a variety of inelastic and elastic collisions. The problem involves solving the linear Boltzmann equation with emphasis on collisions.

Electron transport has also been considered by the magnetospheric community [*Evans*, 1974; *Gurgiolo and Burch*, 1988]. In the magnetosphere, collisions with the neutral gas may be neglected, while the role of electric and magnetic fields becomes important. The equations that describe the dominant physical processes in the magnetosphere differ from those applicable to the atmosphere to the extent that it has not (yet) been possible to couple the two regions self-consistently. We have made a start in this direction by introducing an electric field acceleration term and a converging magnetic field term into the collisional electron transport equation. The magnetic field term simply specifies the dipole field variation, **B**, with altitude. There are two components to the electric field, a polarization field and a field due to current flowing in a region of finite conductivity.

In the atmosphere and ionosphere, elastic and inelastic collisions dominate the processes that govern the phase space distribution of energetic particles as well as the ion composition and density and the plasma temperature. We therefore solve the coupled electron transport, ion continuity, and electron and ion energy equations self-consistently. We do not include Poisson's equation which couples the electric field with the charge density. We cannot, therefore, adopt a self-consistent electric field due to a current of magnetospheric origin. Two parallel electric field models are assumed. In one case the field is linearly increased from the polarization field magnitude at 300 km to a maximum at the upper boundary, while in another case, a uniform field is added to the polarization field. In both cases the electric field term is always a small acceleration source in the transport equation and has no direct influence on the ion and electron continuity and energy equations.

PARALLEL ELECTRIC FIELDS

The large difference in mass between the positive ions and electrons gives rise to a corresponding difference in the inertial force terms in the equations for the diffusion velocity. Separation of oppositely charged species is prevented, however, by the development of a polarization field that constrains the ions and electrons to drift as a single gas, thus maintaining bulk charge neutrality in the ionosphere. For

Paper number 93JA01742.
0148-0227/93/93JA-01742$05.00

most F region applications, collisional interactions dominate over field effects, and Ohm's law reduces to

$$\mathbf{J} = \sigma_e \left[\mathbf{E} + \frac{kT_e}{en_e} \nabla n_e \right] + \tau_e \nabla T_e \tag{1}$$

where σ_e is the electrical conductivity, τ_e is the current flow conductivity due to thermal gradients at constant electron density, $\mathbf{E}$ is the polarization electric field, T_e and n_e are the electron temperature and density, respectively. In the ionosphere, the polarization field $\mathbf{E}$ is determined by the current, $\mathbf{J}$, rather than vice versa:

$$\mathbf{E} = \frac{\mathbf{J}}{\sigma_e} - \frac{kT_e}{en_e} \nabla n_e - \frac{\tau_e}{\sigma_e} \nabla T_e \tag{2}$$

Polarization electric fields exist whenever there are gradients in the electron density and temperature, and field-aligned currents provide an additional component of electric field. A precipitating electron flux contributes to the field-aligned current not only directly but also through enhanced ionisation produced by its interaction with atmospheric gases. In addition, a suprathermal electron stream heats the electron gas, resulting in an increase of the electron temperature. In turn, an upward directed polarization field accelerates the downward moving electrons and decelerates the upward moving component. In this context, downward means the direction from the magnetosphere into the ionosphere along the magnetic field line; upward is in the opposite direction. The perturbed electron energy distribution results from the effects of the polarization field on the ionospheric parameters and, in turn, implies a change in the polarization electric field, that is, the physical processes are coupled. The polarization electric field represents the baseline value of a parallel electric field in the topside ionosphere.

Several processes have been proposed in the literature to show that additional parallel electric fields can be supported self-consistently under various conditions. These mechanisms (reviewed by *Kan* [1982] and *Lundin and Eliasson* [1991]) include anomalous resistivity, double layers, electrostatic shocks, pitch angle anisotropy, magnetic mirror effect on parallel currents, thermoelectric effects, and Alfvén waves. As the accelerated auroral electrons impinge on the atmosphere, ionization and hence the ionospheric conductivity are enhanced. In addition to the loss cone constriction on the upward field-aligned current, anomalous resistivity due to current-driven instabilities can also limit the current and may lead to a potential drop along field lines [*Stasiewicz*, 1984; *Boehm et al.*, 1990]. Observations of upward field aligned ion beams and electric field reversals suggest that the low-altitude boundary of an auroral potential structure may be located below 1000 km [*Mozer*, 1980, 1981].

The electron acceleration mechanisms enumerated above are believed to operate primarily above the thermosphere; however, to close the magnetosphere-ionosphere circuit, the current continuity condition requires the presence of field-aligned currents. Field-aligned currents in the topside ionosphere have been inferred from the perturbations that are produced in the magnetic field [*Evans et al.*, 1977; *Lanchester and Rees*, 1987]. The largest field-aligned current densities in the ionosphere are associated with thin auroral arcs, especially near their edges [*Lanchester and Wallis*, 1985; *McFadden et al.*, 1990]. *Otto and Birk* [1992] have suggested that a resistive instability operates within the ionosphere in regions of sheared magnetic field topology. This proposal is consistent with low-altitude satellite-borne measurements of magnetic field perturbations. The instability can grow under typical ionospheric conditions and is not damped by plasma-neutral gas frictional forces or by ionization/recombination processes. In this paper we investigate the consequences of the parallel electric field that is associated with electron precipitation and auroral arc formation.

ELECTRON TRANSPORT EQUATION

The interaction of suprathermal electrons with the partially ionized gas in the thermosphere is described by the electron continuity equation

$$\frac{\partial f(\mathbf{r},\mathbf{v},t)}{\partial t} + \mathbf{v} \cdot \nabla_r f(\mathbf{r},\mathbf{v},t) + \nabla_v [\dot{\mathbf{v}} f(\mathbf{r},\mathbf{v},t)] = \left(\frac{\delta f(\mathbf{r},\mathbf{v},t)}{\delta t} \right)_{coll} \tag{3}$$

For the treatment of auroral electron transport, a number of approximations can be made to simplify the nonlinear Boltzmann equation in order to arrive at a linear transport equation. The transit time of precipitating electrons along the magnetic field lines is short compared to changes in the atmosphere in response to electron impact. Thus the structure of an auroral potential region is likely to be controlled by its boundary conditions, and auroral electron transport is generally considered to be quasi-static. The explicit time dependence of the electron distribution function is therefore neglected ($\partial f/\partial t = 0$). For the magnetic field strength and average mean free path in the topside ionosphere, the electron gyrofrequency is much larger than the collision frequency. The transport of an individual electron can then be represented by the motion of its guiding center. Consequently, the average motion is symmetric with respect to azimuth and one-dimensional along the geomagnetic field.

The interaction of the streaming electrons with the ambient electron gas is approximated by a continuous energy loss process. The energy loss to the ambient electrons with density n_e is specified by the loss function $L(\epsilon)$ [*Swartz et al.*, 1971]. The total change in momentum is

$$m_e \frac{\partial \mathbf{v}}{\partial t} = -n_e L(\epsilon) \frac{\mathbf{v}}{v} + q\mathbf{E} + q \frac{\mathbf{v} \times \mathbf{B}}{c} \tag{4}$$

where

$$L(\epsilon) = \frac{3.37 \times 10^{-12}}{\epsilon^{0.94} n_e^{0.03} \left(\frac{\epsilon - T_e}{\epsilon - 0.53 T_e} \right)^{2.36}} \tag{5}$$

and T_e is the ambient electron temperature in electron volts, n_e is the electron density in electrons per cubic centimeter, and ϵ is the energy of the incident electrons in electron volts. The electric field is related to the potential drop ϕ by $\mathbf{E} = -\nabla\phi$. The electron energy is $\epsilon = \frac{1}{2} m_e v^2 + q\phi$ and $q = -e$ for electrons.

Following *Stamnes and Rees* [1983], the loss term in equation (4) is transformed, and the continuity equation becomes,

$$\mathbf{v} \cdot \nabla_r f - \frac{m_e}{v} n_e \frac{\partial}{\partial \epsilon} \left(\frac{v^2}{m_e} L f \right) - e(\mathbf{E} + \frac{\mathbf{v} \times \mathbf{B}}{c}) \cdot \mathbf{v} \frac{\partial}{\partial \epsilon} f = \left(\frac{\delta f}{\delta t} \right)_{coll} \tag{6}$$

Conservation of the first adiabatic invariant requires that

$$\frac{\frac{1}{2}m_e v_\perp^2}{B} = \frac{(\epsilon + e\phi)(1-\mu^2)}{B} = \text{constant}$$

where μ is the cosine of the pitch angle. Differentiating with respect to μ yields

$$\mathbf{v}\cdot\nabla_r f = \mu v\frac{\partial f}{\partial s} - \frac{(1-\mu^2)v}{2B}\frac{\partial B}{\partial s}\frac{\partial f}{\partial \mu} - \frac{(1-\mu^2)}{2}\frac{evE}{\epsilon + e\phi}\frac{\partial f}{\partial \mu} \tag{7}$$

where s is a spatial variable along the magnetic field line.

The collision term in the continuity equation, on the right-hand side, specifies the interaction of the electrons with neutral and charged particles in the thermosphere, including elastic, excitation, dissociation, and ionization collision. In each collision an electron is transferred between points in phase space. For each process k we have

$$\frac{v}{m_e}\left(\frac{\delta f}{\delta t}\right)_{coll}^{k} = n(\mathbf{r})\sigma^k(\epsilon')\int p_k(\mu'\to\mu)I(\mathbf{r},\epsilon',\mu')d\mu' - n(\mathbf{r})\sigma^k(\epsilon)I(\mathbf{r},\epsilon,\mu) \tag{8}$$

where n(r) is the neutral density, σ^k is the cross section, and p_k is the phase function of the kth collision process. The first term on the right-hand side constitutes a source of electrons for a phase space volume; the second term is a loss term.

Taking into account elastic and inelastic collisions, the geomagnetic mirror effect through conservation of the first adiabatic invariant, the electric field, and the interaction with ambient electrons through the continuous slowing down approximation and defining the electron intensity $I(s,\epsilon,\mu) = v^2 f(\mathbf{r},\mathbf{v},t)/m_e$ [*Duderstadt and Martin*, 1979], the one-dimensional steady state transport equation is

$$\mu\frac{\partial I}{\partial s} - \frac{(1-\mu^2)}{2B}\frac{\partial B}{\partial s}\frac{\partial I}{\partial \mu} - n_e\frac{\partial(LI)}{\partial \epsilon} - \frac{eE}{2(\epsilon+e\phi)}(1-\mu^2)\frac{\partial I}{\partial \mu} - \mu eE(\epsilon+e\phi)\frac{\partial}{\partial\epsilon}\frac{I}{(\epsilon+e\phi)} = -\sum_j n_j {\sigma_j}^{tot} I + Q^{el} + Q^{ex} + Q^{ion} + Q_{photo} \tag{9}$$

where ${\sigma_j}^{tot}$ is the sum of all loss cross sections. Q^{el}, Q^{ex}, Q^{ion} and Q_{photo} are the sources of elastic collision, excitation, ionization, and photoionization, and the summation is taken over all species j.

In order to solve this integro-differential equation for the electron intensity I as a function of the position s, energy ϵ, and cosine pitch angle μ, we treat the electric field and magnetic field terms as sources and treat the energy loss term as an additional collisionlike process. Denoting the angle between the horizontal and the magnetic field direction by α, the altitude z is given by $z = s\sin\alpha$. Substituting the scattering depth τ for the altitude z by

$$d\tau = -\sum_j (n_j(z)\sigma_j^{tot}(\epsilon) + n_e\frac{L(\epsilon)}{\Delta\epsilon})\frac{dz}{\sin\alpha}$$

we obtain

$$\mu\frac{\partial I(\tau,\epsilon,\mu)}{\partial\tau} = I(\tau,\epsilon,\mu) - \frac{\omega(\tau,\epsilon)}{2}\int_{-1}^{1} p(\epsilon,\mu'\to\mu)I(\tau,\epsilon,\mu')d\mu' + Q_{coll}(\tau,\epsilon,\mu;I) + Q_B(\tau,\epsilon,\mu;I) + Q_B(\tau,\epsilon,\mu;I) \tag{10}$$

where $\Delta\epsilon$ is the energy difference between two energy levels, and $\omega(\tau,\epsilon)$ is the scattering albedo, which is the ratio of the elastic collision frequency to the total collision frequency [*Lummerzheim*, 1987]. Q_{coll} combines all internal sources, including locally produced photoelectrons, energy-degraded electrons from inelastic collisions at higher energies, and secondary electrons from ionizing collisions. Q_B and Q_B are the electric field and the inhomogeneous magnetic field terms.

The solution of this angular dependent electron transport equation requires solving an integro-differential equation by adopting and modifying the discrete ordinate method (DOM) of radiative transfer [*Stamnes et al.*, 1988; *Lummerzheim et al.*, 1989] and evaluating the source functions Q_{coll}, Q_B, and Q_B.

Energy degradation is handled by solving the problem from high to low energies. The component of Q_{coll} due to energy-degraded electrons at a given energy can be computed from the intensity distribution at higher energies. Q_B and Q_B depend not only on $\frac{\partial}{\partial\epsilon}$ but also on $\frac{\partial}{\partial\mu}$. The DOM method of *Stamnes et al.* [1988] provides analytic expressions for the intensity which can be evaluated at any desired angle. The derivative with respect to angle is

$$\frac{\partial I(\tau,\epsilon,\mu)}{\partial\mu} \approx \frac{I(\tau,\epsilon,\mu+\delta\mu) - I(\tau,\epsilon,\mu)}{\delta\mu}$$

and we use a finite difference scheme to calculate the energy derivative:

$$\frac{\partial I(\tau,\epsilon,\mu)}{\partial\epsilon} \approx \frac{I(\tau,\epsilon_{n+1},\mu) - I(\tau,\epsilon_n,\mu)}{\epsilon_{n+1}-\epsilon_n}$$

We restrict our attention to examining weak upward electric fields with a strength below 50 μV/m. In this range the energy gained by an electron in a mean free path at heights less than 1000 km does not exceed the mean energy of thermal electrons. This obviates the need to include wave processes associated with the excitation of low-frequency plasma instabilities.

The downward electron intensity is specified at the upper boundary, while the upward electron intensity is given at the lower boundary. The lower boundary is assumed to lie at a density within the atmosphere that is large, so that the intensity becomes vanishingly small. The upper boundary condition applied to the transport equation depends on the problem that is being addressed. In the photoelectron transport case we assume a small downward electron flux characterized by a Maxwellian energy distribution with a characteristic energy of about 50 eV and an energy flux of

0.03 ergs $cm^{-2}s^{-1}$ to account for the contribution from the conjugate hemisphere. In the auroral case the flux also vanishes at the lower boundary, while at the upper boundary, we specify the intensity of auroral electron precipitation derived from rocket or satellite measurements or of an assumed analytic form.

The energy steps adopted in the numerical solution of equation (10) are sufficiently close together to justify specifying the source terms due to the electric and magnetic fields at a given energy by their value at the next higher energy on the grid. We have verified the validity of this assumption by applying an entirely different method of solution to identical test cases. *Cannon* [1984] has suggested that terms proportional to $\frac{\partial}{\partial \mu}$ and $\frac{\partial}{\partial \epsilon}$ can be treated as nonlocal perturbations. The perturbation method yields values similar to the method which we have adopted, but more than 10 iterations are required to achieve the same results.

SELF-CONSISTENT FIELD-ALIGNED ELECTRIC FIELD

The polarization field given by equation (2) must be consistent with the parameters adopted in the solution of the transport equation. These are the neutral atmosphere and height profiles of the electron density and temperature.

An empirical model is adopted for the neutral atmospheric composition, density, and temperature: the mass spectrometer/incoherent scatter (MSIS) model. Profiles of ionization and electron temperature are computed for two cases, an embedded photoelectron source and an auroral flux of energetic electrons incident at the top of the atmosphere. Several investigators have solved the time dependent ion continuity equations relevant to this problem [e.g., *Dalgarno et al.*, 1969; *Schunk and Walker*, 1970; *Walker and Rees*, 1968; *Jones and Rees*, 1973; *Roble and Rees*, 1977; *Min*, 1993]. The method is described in detail by *Rees* [1989] and is only briefly sketched below.

The coupled continuity equations for all the ion species, i, must be solved as

$$\frac{\partial N_i}{\partial t} = \eta_d^i + \eta_c^i - N_i L_c - \frac{\partial \Phi_i}{\partial z} \tag{11}$$

N_i is the concentration of species i at altitude z, η_d^i and η_c^i are the production rates of species i from direct ionization and from chemical reactions, respectively, and L_i is the local chemical (and radiative) loss rate. The flux due to ambipolar diffusion is Φ_i:

$$\Phi_i = -N_i D_i \left(\frac{1}{N_i} \frac{\partial N_i}{\partial z} + \frac{\partial}{\partial z} \ln T_p + H_i \right) \tag{12}$$

where the ambipolar diffusion coefficient is

$$D_i = \frac{kT_r}{m_i \nu_{in}} \left(1 + \frac{T_e}{T_r} \right) \tag{13}$$

The plasma temperature, T_p, and the reduced temperature, T_r, are

$$T_p = \frac{(T_e + T_i)}{2} \quad , \quad T_r = \frac{(T_i + T_n)}{2} \tag{14}$$

Here ν_{in} is the ion-neutral collision frequency, and the plasma scale height is

$$H_i = \frac{m_i g}{2kT_p} \tag{15}$$

In the altitude region of interest, the F region and above, the major ions are O^+ and H^+, and we solve the coupled diffusion equations for these species. O_2^+, N_2^+, N^+, and NO^+ densities are assumed to have only local sources and sinks, eliminating the flux divergence term in the continuity equations. The chemical reactions included here are listed by *Rees* [1989]. Bulk charge neutrality prevails in the ionosphere; having calculated the ion densities, the electron density is

$$n_e(z) = \sum_i N_i(z) \tag{16}$$

Several reaction rate coefficients are temperature dependent, requiring the continuity equations to be coupled with the energy equations for the electron and ion gas. Solution of the energy equations yields the electron and ion temperatures.

The transit time of auroral electrons and photoelectrons in the thermosphere is short by comparison with changes in the host medium in response to the electron fluxes. The steady state electron energy equation therefore suffices:

$$\sin^2 \alpha \frac{\partial}{\partial z} \left[K^e \frac{\partial T_e}{\partial z} \right] + Q_e - L_e = 0 \tag{17}$$

K^e is the electron thermal conductivity, Q_e is the electron heating rate, and L_e is the cooling rate. The contribution of the thermoelectric current to the heat flow has been neglected. Equation (17) has been discussed in detail by *Rees and Roble* [1975], *Schunk and Nagy* [1978], and *Rees* [1989]. These authors also give numerical values for the conductivity coefficient and numerous contributions to the electron cooling rate L_e. In the upper F region there is substantial exchange of energy between ions and electrons through Coulomb collisions. The ion energy equation

$$Q_{ie} + Q_{E_\perp} - L_{in} = 0 \tag{18}$$

is therefore coupled into the system of equations to be solved. Q_{ie} is the ion heating rate by Coulomb collisions with electrons (an energy loss process for the electron gas), $Q_{E_\perp}$ identifies the joule heating rate, and L_{in} is the ion cooling rate by elastic and inelastic collisions with neutrals. Conduction in the ion gas is negligibly small in the ionosphere, and all ions are assigned the same temperature, T_i, an adequate assumption for our purpose. For the auroral case we have adopted an arbitrary value of 30 mV/m for the orthogonal electric field, providing a small value for the joule heating rate. Details and numerical values for Q_{ei} and L_{in} are given by *Rees and Roble* [1975], *Schunk and Nagy* [1978], and *Rees* [1989].

The ambient electron gas is heated by thermalising elastic collisions with photoelectrons and auroral electrons. The heating rate in equation (17) is given by

$$Q_e = \int_{\epsilon_0}^{\infty} \int_{-1}^{1} n_e(z) L(\epsilon) I(z, \epsilon, \mu) \, d\epsilon \, d\mu \tag{19}$$

where ϵ_0 is the thermal energy, $L(\epsilon)$ is the electron loss function (equation (5)), and $I(z, \epsilon, \mu)$ is the electron intensity (equation (10)). Equation (19) expresses the coupling between electron transport, continuity, and electron energy equations. Part of the energy brought into the atmosphere by photoelectron and auroral electron fluxes is shared with the ambient electron gas, raising its temperature above that of the neutral gas.

The differential equation (17) requires boundary conditions appropriate to the physical problem being investigated. Local equilibrium prevails at the lower boundary. A heat flux is appropriate at the upper boundary, but observations provide little guidance. More commonly, the heat flux is adjusted to match a measured temperature. Large heat fluxes produce temperature gradients that influence the magnitude of the polarization field. Large values of heat flux are associated with the decay of the ring current during large geomagnetic storms. The resulting high electron temperature, in excess of 6000 K, accounts for the midlatitude red arc phenomenon associated with such events [*Rees and Roble*, 1975]. We have assumed a downward heat flux of 1×10^9 eV cm^{-2} s^{-1} which yields values of T_e typically measured during auroral activity.

The polarization electric field, equation (2), has three contributions that arise from the electron density and electron temperature gradients and from a field-aligned current. If the field-aligned current is attributed to the flow of suprathermal (i.e., auroral and photoelectron) electrons only and the parallel conductivity is assumed to be due to collisions,

$$\sigma_e = \frac{e^2 n_e}{m_e(\nu_{en} + \nu_{ei})} \tag{20}$$

then the $\mathbf{J}/\sigma_e$ term is small compared with the gradient terms. The electron-neutral and electron-ion collision frequencies are ν_{en} and ν_{ei}, respectively. Measurements of the geomagnetic field perturbations in the topside auroral ionosphere have shown, however, that the actual current may be much larger than the auroral electron stream would suggest, implying the presence of a substantial thermal component of the current. If an "anomalous" resistance is present in the topside ionosphere under auroral precipitation conditions, then the contribution of the current term to the parallel electric field may be much larger than the minimum associated with the polarization effect. We will discuss this possibility by adding an arbitrary parallel electric field to equation (2). For the purpose of this study we assume that this field is maintained by the field-aligned auroral currents in the vicinity of an auroral arc. Such fields will perturb the thermal balance in the ionospheric electron gas, but in this paper we focus on the effects of the parallel field on the electron energy distribution function. Joule heating from parallel electric fields of the magnitude adopted here is negligibly small.

NUMERICAL RESULTS

To evaluate the consequences of a parallel electric field and the Earth's dipole magnetic field on the energy distribution of electron fluxes, we have carried out numerical calculations of the coupled electron transport, ion continuity, and energy equations for an auroral event representing an external flux source and for a solar case representing an embedded source of photoelectrons. We present the auroral case first.

We adopted the MSIS-90 neutral atmosphere [*Hedin*, 1991] at 60°N, 200°E for northern winter (year 1990, day 030). We assumed an $F_{10.7}$ solar activity index of 150 and an *Ap* index of 30. The model run was started at noon, but the auroral precipitation was not turned on until 2200 LT. Auroral electron precipitation was simulated by an isotropic angular distribution and a Maxwellian energy distribution with 1-keV characteristic energy and a 5 ergs cm^{-2} s^{-1} energy flux, supplemented by a power law spectrum with energy dependence ϵ^{-2} below 100 eV. The auroral electron flux is imposed at the upper boundary at 800 km. Our model covers the region between 80 and 800 km. At the lower boundary of 80 km, zero backscattered flux is assumed in the transport equation, photochemical equilibrium is assumed in the continuity equations, and equal electron, ion, and neutral temperatures are assumed in the energy equations. Our assumed input parameters and boundary conditions are representative of observed auroral events [c.f. *Winningham et al.*, 1977; *Pulliam et al.*, 1981; *Lummerzheim et al.*, 1989].

The self-consistent polarization field associated with the auroral event specified above and computed from equation (2) is shown in Figure 1. The dominant term is the electron density gradient, yielding an upward directed field of about 3 μV/m at 350 km and a near-constant value of 1.5 μV/m above 500 km. The temperature gradient term produces a downward directed field, since the gradient is positive at all altitudes. The electric field due to the current density term is small and directed upward. Only the current carried by the energetic flux is included in this term which is smaller than the field-aligned current inferred from measurements of magnetic field perturbations recorded by instruments on board satellites and rockets overflying auroral arcs [c.f. *Lanchester and Wallis*, 1985; *Lanchester and Rees*, 1987]. A reversal, to a downward directed $\mathbf{E}_\parallel$, occurs at about 200 km, but this has no effect on the electron intensity distribution which is controlled entirely by collisional interactions below about 300 km.

The differential electron flux computed from our model aurora is shown in Figure 2 at 800, 400, and 200 km. The downward flux at 800 km is the imposed boundary value, but the upward flux is the result of elastic and inelastic collisions, as well as the polarization electric field and dipole magnetic

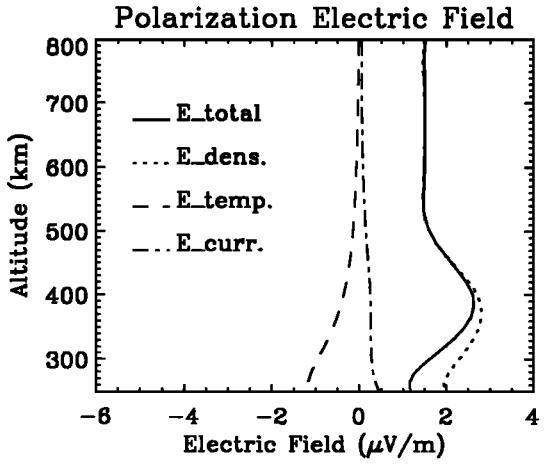

Fig. 1. Altitude profile of the polarization field for the auroral case presented in the text. The total field as well as terms corresponding to the density gradient, temperature gradient, and current are shown. Positive values signify upward directed fields.

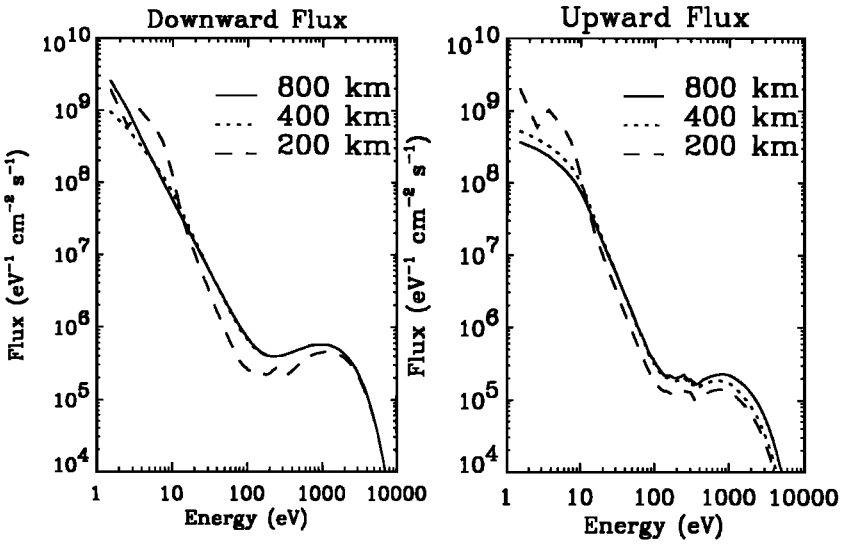

Fig. 2. Differential auroral electron fluxes for an assumed downward input flux at 800 km. The computed downward and upward hemispheric fluxes are shown at three altitudes.

field. Collisional and field effects contribute to the evolution of the distribution with increasing atmospheric depth, and we note that at 200 km, the downward and upward components of the flux are virtually identical up to energies of several tens of electron volts. The structure at 2 to 3 eV is attributed to the large cross section for excitation of vibrational levels in N_2, but the effect becomes pronounced only at levels where molecular species become abundant. We use the extensive compilation of cross sections and phase functions assembled by *Lummerzheim* [1987] in our electron transport model. The transport equation is solved using four streams. To assess the contributions of fields to the structure of the differential fluxes, we have repeated the calculations under five different assumptions: (1) no magnetic field gradient and no polarization field, (2) no magnetic field gradient and a self-consistent $E_{\parallel}$, (3) a dipole magnetic field and a self-consistent $E_{\parallel}$ (leading to the results in Figure 2), (4) a dipole magnetic field and an $E_{\parallel}$ consisting of the polarization field and an additional 20 μV/m applied uniformly, and (5) a dipole magnetic field and an $E_{\parallel}$ consisting of the polarization field and an additional field that increases linearly from 0 to 40 μV/m between 300 and 800 km. The results are displayed in different ways in Figures 3 and 4. The downward and upward directed hemispherical fluxes are shown in Figures 3*a* and 3*b* at 800 km and 400 km, respectively, to illustrate the different effects of the magnetic and electric fields. At 800 km the downward flux is the imposed boundary condition, while the upward flux shows the effect of deceleration by the parallel electric field at electron energies below 100 eV. The magnetic mirror force has the effect of increasing the upward flux at electron energies above a few hundred electron volts. The 400-km altitude regime is closer to the embedded source of secondary electrons, and the decelerating effect of the electric field is offset by the increased source term. The collision terms likewise tend to decrease the field effects. Even so, the enhanced parallel electric field effectively increases the low-energy portion of the electron flux. Figure 4 illustrates the same point. The downward component of the 2-keV flux is unperturbed over the entire altitude range, while the upward flux shows the effect of the magnetic mirror force above about 300 km. The factor of 2 increase at 800 km in the backscattered flux should produce effects such as electron heating and enhancement of optical emissions that may be observed. The parallel electric field is entirely responsible for perturbations in the 10-eV electron flux. Profiles of the upward and downward fluxes, shown in Figure 4*b*, illustrate the combined effects of the embedded source region, the accelerating/decelerating electric field, and the elastic and inelastic scattering processes. For different boundary conditions, that is different electron fluxes at the top of the atmosphere, the contribution of the various terms in the transport equation will, of course, differ from the case illustrated in Figures 4*a* and 4*b*.

Observations of large parallel current densities at edges of auroral arc structures suggest the development of parallel electric fields due to nonohmic resistance [*Papadopoulos*, 1977, *Stasiewicz*, 1984]. We have investigated the consequences of imposing both a uniform and a linearly increasing upward directed parallel electric field, in addition to the self-consistent polarization field; magnitudes of 10 and 15 μV/m for the uniform and 0 to 20 and 0 to 30 μV/m for the linearly increasing field were adopted. Since the largest effect of an $E_{\parallel}$ is on the electron flux below 100 eV, we show the results of our computations in the energy range between 3 and 100 eV. The curves in Figures 5*a* and 5*b* essentially expand upon the results shown in Figures 3*a* and 3*b*: the downward flux at the upper boundary of 800 km is given (and not shown in the figure), while the upward moving electrons are decelerated; the upward flux is also decelerated at 400 km, but this term is overshadowed by the embedded source and scattering terms; the downward flux at 400 km undergoes substantial acceleration, increasing the 3-eV flux by a factor of more than 2 for the 30-μV/m linearly increasing electric field. Height profiles of the 10-eV downward and upward fluxes are shown in Figure 6. A substantial enhancement in the omnidirectional flux between 250 and 600 km is shown for the 0- to 30-μV/m linearly increasing parallel electric field. At the altitude at which the upper boundary is imposed, the downward flux shown in the figure is not realistic. More likely, the increase in the flux under the influence of an $E_{\parallel}$ should persist at the boundary. The same point applies to the downward flux at 800 km shown in Figure 4*b*.

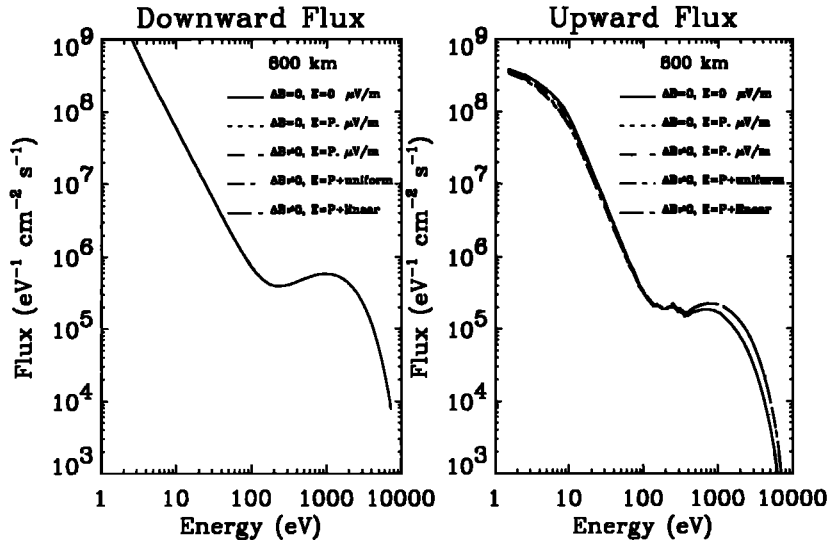

Fig. 3a. Electron energy spectra of downward and upward hemispheric fluxes at 800 km for five different cases: no electric field and a homogeneous magnetic field (solid lines), a polarization field and a homogeneous magnetic field (dotted lines), a polarization field and a divergent magnetic field (dashed lines), a polarization field plus a uniform electric field of 20 μV/m and a divergent magnetic field (dash-dotted lines), and a polarization field plus a field that linearly increases from zero at 300 km to 40 μV/m at 800 km and a divergent magnetic field (dash-triple-dotted lines).

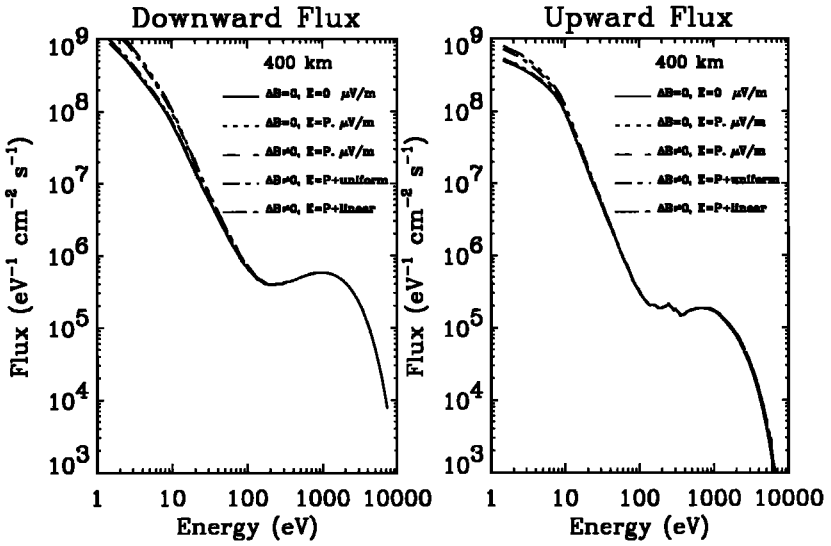

Fig. 3b. The electron energy spectra of downward and upward hemispheric fluxes at 400 km for the same cases as in Figure 3a.

However, deceleration of the upward flux may result in little change of the omnidirectional flux.

Discussion of the Auroral Case

The omnidirectional electron flux is the parameter that accounts for auroral ionization, plasma temperature enhancements, and auroral spectral emission features. Optical emissions do not influence the electron flux; the energy is radiated out of the region of excitation. Ionization and the electron temperature appear in various terms of the transport equation, necessitating the coupled solutions of the transport, continuity, and energy equations described above. The electron density and electron temperature profiles obtained by including the self-consistent polarization field in the coupled solution are shown in Figure 7 for the auroral case described in the preceding section. The electron density profile is influenced very little by a parallel field. This is to be expected because ionization cross sections have maxima between about 100 eV and 200 eV, and in this energy range the electron flux is not significantly perturbed by the electric field. Heating of the ambient electron gas is most efficient in collisions with low-energy auroral electrons (c.f. equation 5) and it is this population that is most sensitive to the influence of electric fields. However, in the presence of large parallel electric fields the electron gas is also heated by noncollisional plasma effects, and equation (5) no longer provides the sole source of heating. A downward heat flux from the magnetosphere also contributes to electron heating. The electron temperature cannot be computed without quantitative knowledge of all heat sources.

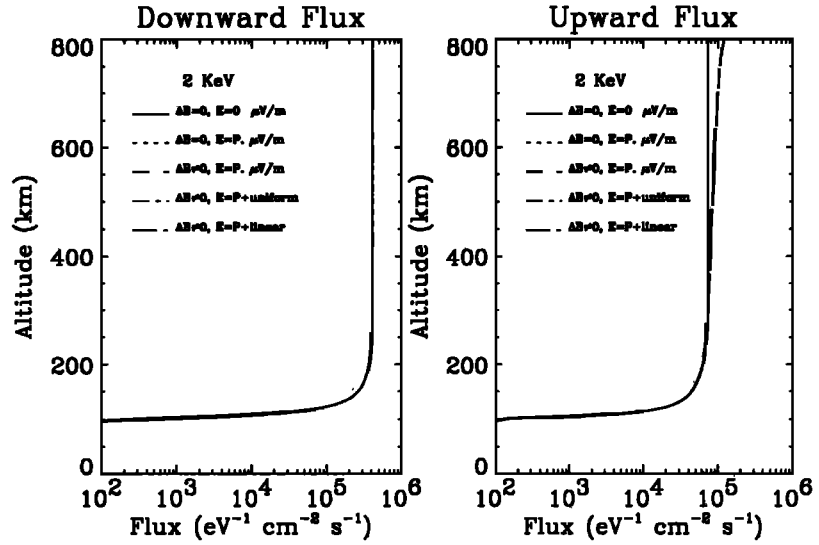

Fig. 4*a*. Altitude profiles of the downward and upward hemispheric fluxes of 2-keV electrons for the five different cases shown in Figure 3*a*.

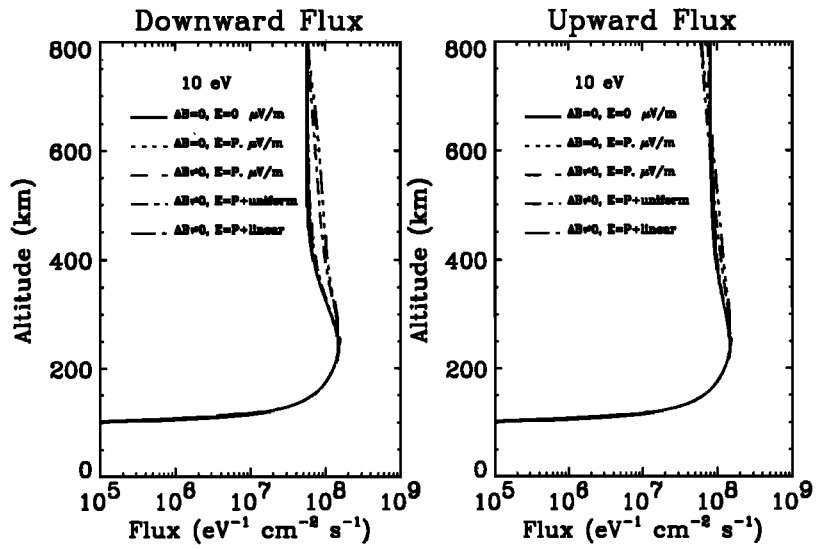

Fig. 4*b*. Altitude profiles of the downward and upward hemispheric fluxes of 10-eV electrons for the same five cases shown in Figure 3*a*.

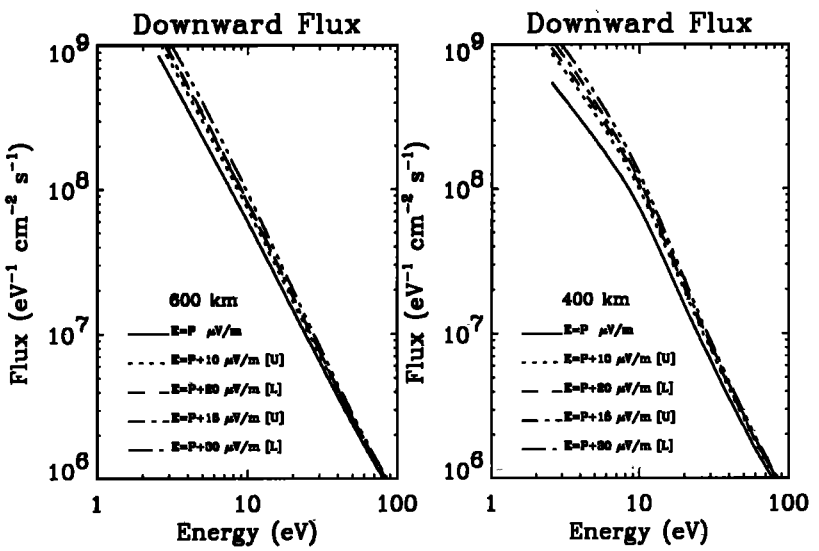

Fig. 5*a*. Electron energy spectra between 3 and 100 eV of the downward hemispheric flux at 600 km and 400 km for the auroral example described in the text. Results are shown for the baseline polarization electric field (labeled E = P) and four models of enhanced parallel electric fields: polarization plus a uniform 10-μV/m field, polarization plus a linearly increasing 0- to 20-μV/m field, polarization plus a uniform 15-μV/m field, and polarization plus a linearly increasing 0- to 30-μV/m field.

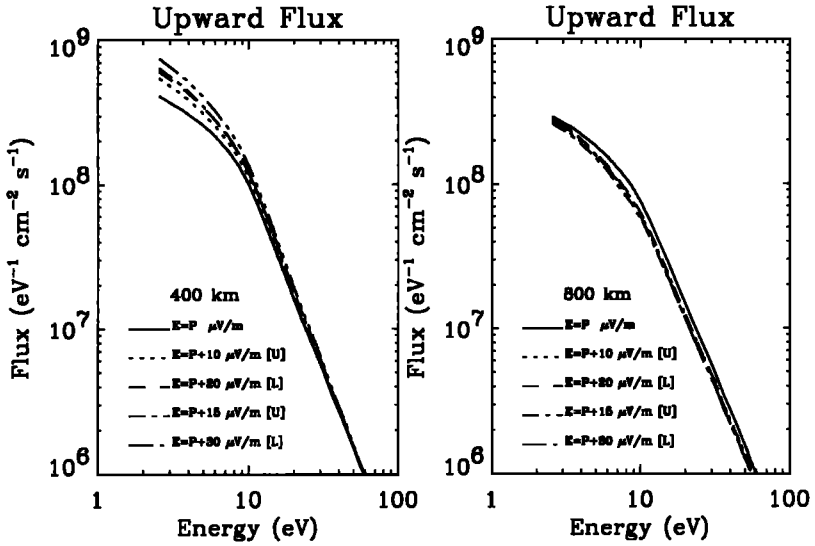

Fig. 5*b*. Electron energy spectra between 3 and 100 eV of the upward hemispheric flux at 800 km and 400 km for the cases shown in Figure 5*a*.

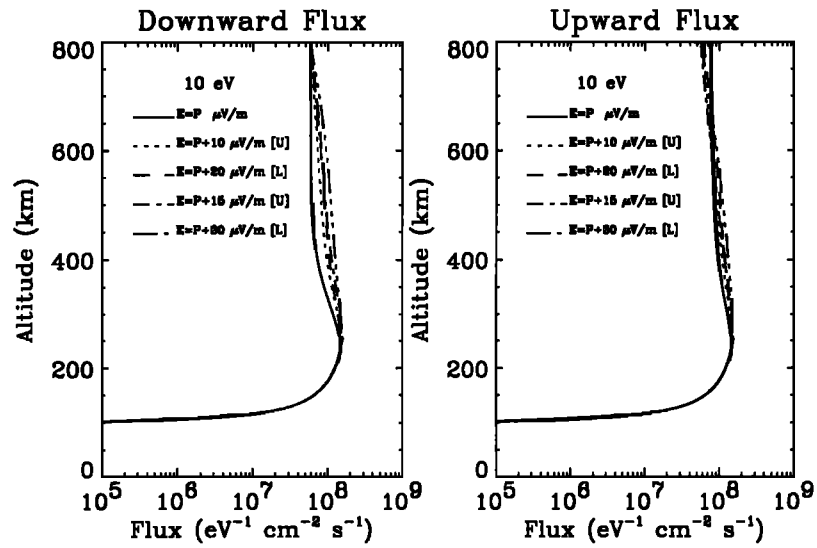

Fig. 6. Altitude profiles of the downward and upward hemispheric fluxes of 10-eV electrons for the different models of the parallel electric field described in Figure 5*a*. The behavior of the downward flux at the upper boundary is discussed in the text.

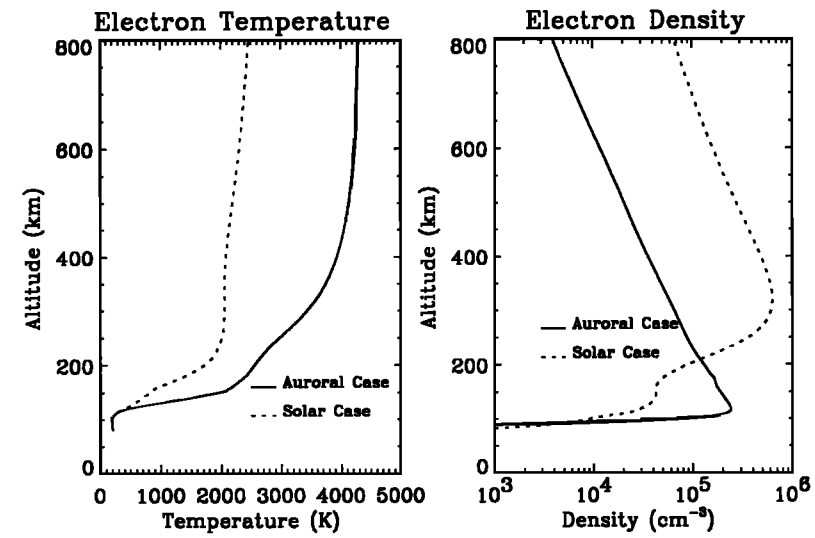

Fig. 7. Altitude profiles of electron density and temperature for the auroral and solar cases that include the polarization electric field and a divergent magnetic field.

Excitation thresholds of several prominent auroral emission features lie in the energy regime of a few electron volts, notably the $O(^1D)$ and $O(^1S)$ states and the $N(^2D)$ and $N(^2P)$ states. Electron impact is an important source of $O(^1D)$, and its excitation rate is directly proportional to the magnitude of the electron flux. A parallel electric field may, therefore, substantially increase the excitation rate of $O(^1D)$ at an altitude where collisional deactivation is minimal. An increase of the electron temperature further enhances excitation of $O(^1D)$. While thermal excitation has been included in current models of the 6300-Å emission, the enhancement of the low-energy electron flux by a parallel electric field has not been included and could be substantial.

An enhanced flux of secondary auroral electrons due to a parallel electric field may help to account for auroral observations that have, to our knowledge, remained unexplained. *Störmer* [1955, Figure 90] gives examples of auroral rays that extend as high as 600 km in the nonsunlit atmosphere (sunlit aurorae occur even higher). The problem involves obtaining an excitation rate that is sufficient to produce observable aurora (visually and photographically in Störmer's data). The excitation rate at altitude z is

$$q^{e*}(z) = n(z) \int_\epsilon \sigma^{e*}(\epsilon) I(\epsilon, z)\, d\epsilon \qquad (21)$$

where $n(z)$ is the number density of neutral species that are excited, $\sigma^{e*}(\epsilon)$ is the energy dependent excitation cross section, and $I(\epsilon, z)$ is the omnidirectional electron intensity. Auroral electrons penetrate through the low-density region of the atmosphere without depositing much energy locally. An appreciable intensity, therefore, depends on the backscattered (upward) component and an enhanced downward component due to a parallel electric field (Figure 5). It is likely that during a large geomagnetic storm, the atmosphere is heated and expands to increase the neutral density at a given altitude. Excitation cross sections are now better known than they were in Störmer's time. We now need calibrated auroral observations of very high nonsunlit auroral rays to investigate the proposed hypothesis.

EFFECT OF $E_\parallel$ ON PHOTOELECTRON FLUXES

The source of photoelectrons is embedded in the atmosphere, supplemented by a small external flux from the conjugate hemisphere. We investigate the effects of the polarization electric field on the photoelectron flux in the absence of any auroral precipitation. Several investigators have solved the photoelectron transport problem [e.g. *Banks and Nagy*, 1970; *Oran and Strickland*, 1978; *Link*, 1992], but none have included a self-consistent polarization field. We have compared our photoelectron source and transport calculation to the results of previously published photoelectron transport calculations [*Meier et al.*, 1985; *Link*, 1992] and found good agreement.

We use a photoelectron production code developed by *Lilensten* [1989] to generate the source function at a solar zenith angle of 87° at 1510 LT. Like other investigators, we adopt the solar EUV spectra from *Hinteregger* [1981] for solar maximum and solar minimum conditions and interpolate between them assuming a linear dependence of the spectral EUV flux on the $F_{10.7}$ flux. These EUV spectra have a lower cutoff at 30 Å, and thus our source of photoelectrons is limited to 224 eV. Following the conclusions of *Winningham et al.* [1989], we include a small conjugate photoelectron flux by specifying a downward flux of 0.03 erg cm^{-2} s^{-1} with a characteristic energy of 50 eV at the upper boundary. Solving the coupled electron transport, ion continuity, and energy equations as previously described, we obtain the height profile of the polarization electric field shown in Figure 8. The upward directed field is almost constant above 400 km at a level of about 1 μV/m. The major contribution is due to the electron density gradient term.

The downward and upward components of the photoelectron flux are shown in Figure 9 at three altitudes. Comparison with Figure 2 (the auroral case) shows the difference produced by the embedded source which attains a maximum at about 200-km altitude. We note that the upward flux at 800 km in the 10- to 40-eV energy region exceeds the downward flux by 1 order of magnitude to become a source of conjugate photoelectrons. The result of solving the coupled governing equations shows that the contributions of various terms (sources, sinks, elastic scattering, inelastic processes, polarization field, dipole magnetic field, etc.) makes it virtually impossible to predict by hand-waving arguments the evolution of the electron flux with altitude. Detailed transport calculations coupled with the ion chemistry and energetics are required to model the response of the atmosphere to solar ionization.

Figure 10 shows that photoelectron fluxes that are computed with our model including the self-consistent parallel electric field and photoelectron fluxes that are computed without including the effects of this field exhibit only small differences. Uncertainties in the solar EUV flux outweigh these changes of the photoelectron flux. The electron density and electron temperature profiles obtained for this solar case by solving the coupled transport, continuity, and energy equations are shown in Figure 7.

CONCLUSIONS

The effects of a parallel electric field and the geomagnetic field on auroral electron and photoelectron distributions in the topside ionosphere have been investigated. This has

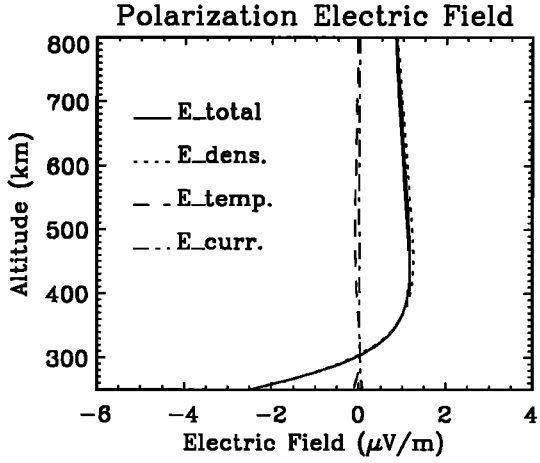

Fig. 8. Altitude profiles of the polarization field for the photoelectron case. The total field as well as terms corresponding to the density gradient, temperature gradient, and current are shown. Positive values signify upward directed fields.

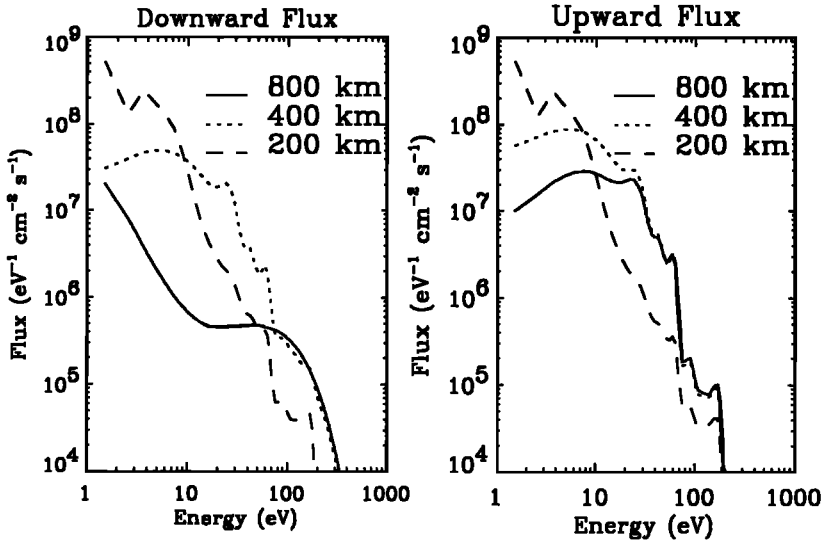

Fig. 9. Differential photoelectron energy spectra of the downward and upward hemispheric fluxes at three altitudes.

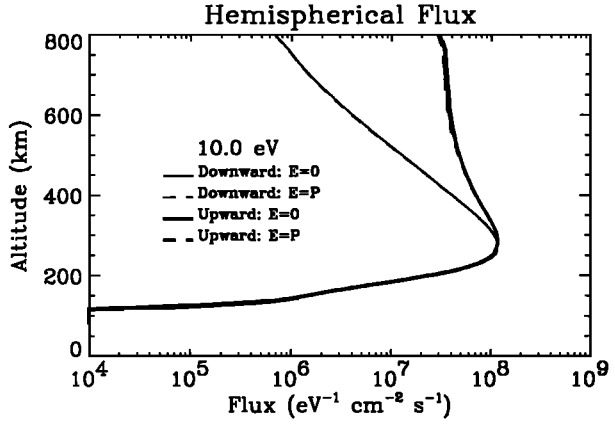

Fig. 10. Altitude profiles of the downward and upward hemispheric fluxes of 10-eV photoelectrons with and without the self-consistent polarization electric field.

been accomplished by self-consistently solving the coupled electron transport, ion continuity, and electron and ion energy equations. Field effects are important when electrons experience a significant change in energy and/or momentum in a mean free path between collisions. Computations show that

1. Electric fields are most effective in perturbing the low-energy ($\epsilon < 50$ eV) component of the electron distribution function.

2. Electric and magnetic fields of the magnitude investigated in this work perturb the distribution functions at altitudes above about 250 km but not below.

3. The polarization electric field (above 250 km) and the field due to field aligned currents are directed upward, thus accelerating the downward electron flux and decelerating the upward component. Two models of enhanced parallel electric fields are investigated: a uniform field representing a parallel plate capacitor and a field that linearly increases from zero in the F region to a finite value at the upper boundary.

4. The inhomogeneous magnetic field produces anisotropies in the angular distribution of the electron intensity that result in perturbations of the high-energy component of the electron distribution function.

5. Excited states of atoms and molecules with electron impact cross sections that maximize at low energies are expected to be enhanced by the presence of parallel electric fields.

Acknowledgments. This research was supported by the National Science Foundation under grant ATM 9022197 and by the National Aeronautics and Space Administrations under grants NAG5-1097 and NAGW-3037.

The Editor thanks J. R. Jasperse and C. A. Gurgiolo for their assistance in evaluating this paper.

REFERENCES

Banks, P. M., and A. F. Nagy, Concerning the influence of elastic scattering upon photoelectron transport and escape, *J. Geophys. Res.*, *75*, 1902, 1970.

Berger, M. J., S. M. Seltzer, and K. Maeda, Energy deposition by auroral electrons in the atmosphere, *J. Atmos. Terr. Phys.*, *32*, 1015, 1970.

Boehm, C. W., C. W. Carlson, J. P. McFadden, and F. S. Mozer, Dual sounding rocket observations of low-altitude electrostatic shocks, *J. Geophys. Res.*, *95*, 12,173, 1990.

Cannon, C. J., Nonlocal perturbation techniques in radiative transfer, in *Methods in Radiative Transfer Problems*, edited by W. Kalkofen, p. 155, Cambridge University Press, New York, 1984.

Dalgarno, A., M. B. McElroy, and A. I. Stewart, Electron impact excitation of the dayglow, *J. Atmos. Sci.*, *2b*, 753, 1969.

Duderstadt, J. J., and W. R. Martin, *Transport Theory*, John Wiley, New York, 1979.

Evans, D. S., Precipitating electron fluxes formed by a magnetic field aligned potential difference, *J. Geophys. Res.*, *79*, 2853, 1974.

Evans, D. S., N. C. Maynard, J. Troim, T. Jacobson, and A. Egeland, Auroral particles and fields, *J. Geophys. Res.*, *82*, 2235, 1977.

Gurgiolo, C., and J. L. Burch, Simulation of electron distributions within auroral acceleration regions, *J. Geophys. Res.*, *93*, 3989, 1988.

Hedin, A. E., Extension of the MSIS thermosphere model into the middle and lower atmosphere, *J. Geophys. Res.*, *96*, 1159, 1991.

Hinteregger, H. E., Representations of solar EUV fluxes for aeronomical applications, *Adv. Space Res.*, *1*, 39, 1981.

Jasperse, J. R., Electron distribution function and ion concentrations in the Earth's lower ionosphere from Boltzmann-Fokker-Planck theory, *Planet. Space Sci., 25*, 1, 1977.

Jones, R. A., and M. H. Rees, Time dependent studies of the aurora—I. Ion density and composition, *Planet. Space Sci., 21*, 537, 1973.

Kan, J. R., Towards a unified theory of discrete auroras, *Space Sci. Rev., 31*, 71, 1982.

Lanchester, B. S., and M. H. Rees, Field-aligned current reversals and fine structure in a dayside auroral arc, *Planet. Space Sci., 35*, 759, 1987.

Lanchester, B. S., and D. D. Wallis, Magnetic field disturbances over auroral arcs observed from Spitsbergen, *J. Geophys. Res., 90*, 2473, 1985.

Lilensten, J., Résolution de l'equation de transport de Boltzmann et applications dans le plasma ionosphérique, Ph.D. thesis, Inst. Nat. Polytech. de Grenoble, Grenoble, France, 1989.

Link, R., Feautrier solution of the electron transport equation, *J. Geophys. Res., 97*, 159, 1992.

Lummerzheim, D., Electron transport and optical emissions in the aurora, Ph.D. thesis, Univ. of Alaska, Fairbanks, 1987.

Lummerzheim, D., M. H. Rees, and H. R. Anderson, Angular dependent transport of auroral electrons in the upper atmosphere, *Planet. Space Sci., 37*, 109, 1989.

Lundin, R., and L. Eliasson, Auroral energization processes, *Ann. Geophys., 9*, 202, 1991.

Mantas, G. P., Theory of photoelectron thermalization and transport in the ionosphere, *Planet. Space Sci., 23*, 337, 1975.

McFadden, J. P., C. W. Carlson and M. H. Boehm, Structure of an energetic narrow discrete arc, *J. Geophys. Res., 95*, 6533, 1990.

Meier, R. R., R. R. Conway, D. E. Anderson Jr., P. D. Feldman, R. W. Eastes, E. P. Gentieu, and A. B. Christensen, The ultraviolet dayglow at solar maximum, 3, Photoelectron-excited emissions of N_2 and O, *J. Geophys. Res., 90*, 6608, 1985.

Min, Q.-L., A self-consistent time varying auroral model, Ph.D. thesis, Univ. of Alaska, Fairbanks, 1993.

Mozer, F. S., On the lowest altitude S3-3 observations of electrostatic shocks and parallel electric fields, *Geophys. Res. Lett., 7*, 1097, 1980.

Mozer, F. S., The low altitude electric field structure of discrete auroral arcs, in *Physics of Auroral Arc Formation, Geophys. Monogr. Ser.*, Vol. 25, edited by S.-I. Akasofu and J. R. Kan, p. 136, AGU, Washington, D.C., 1981.

Nagy, A. F. and P. M. Banks, Photoelectron fluxes in the ionosphere, *J. Geophys. Res, 75*, 6260, 1970

Oran, E. S., and D. J. Strickland, Photoelectron flux in the Earth's ionosphere, *Planet. Space Sci., 26*, 1161, 1978.

Otto, A., and G. Birk, The dynamical evolution of small-scale auroral arc phenomena due to a resistive instability, *J. Geophys. Res., 97*, 6500, 1992.

Papadopoulos, K., A review of anomalous resistivity for the ionosphere, *Rev. Geophys., 15*, 113, 1977.

Porter, H. S., F. Varosi, and H. G. Mayr, Iterative solution of the multistream transport equation, 1, Comparison with laboratory beam injection experiments, *J. Geophys. Res., 92*, 5933, 1987.

Pulliam, D. M., H. R. Anderson, K. Stamnes, and M. H. Rees, Aurora electron acceleration and atmospheric interactions, *J. Geophys. Res., 86*, 2397, 1981.

Rees, M. H., *Physics and Chemistry of the Upper Atmosphere*, Cambridge University Press, New York, 1989.

Rees, M. H., and R. G. Roble, Observations and theory of the formation of stable auroral red arcs, *Rev. Geophys., 13*, 201, 1975.

Roble, R. G., and M. H. Rees, Time-dependent studies of the aurora: Effects of particle precipitation on the dynamic morphology of ionospheric and atmospheric properties, *Planet. Space Sci., 25*, 991, 1977.

Schunk, R., and A. F. Nagy, Electron temperatures in the *F* region of the ionosphere: Theory and observations, *Rev. Geophys., 16*, 355, 1978.

Schunk, R., and J. C. G. Walker, Transport properties of the ionospheric electron gas, *Planet. Space Sci., 18*, 1535, 1970.

Stamnes, K., Analytic approach to auroral electron transport and energy degradation, *Planet. Space Sci., 28*, 427, 1980.

Stamnes, K., On the two-stream approach to electron transport and thermalization, *J. Geophys. Res., 86*, 2405, 1981.

Stamnes, K., and M. H. Rees, Inelastic scattering effects on photoelectron spectra and ionospheric electron temperature, *J. Geophys. Res., 88*, 6301, 1983.

Stamnes, K., W. J. Wiscombe, S. C. Tsay, and K. Jayaweera, An improved, numerically stable multiple scattering algorithm for discrete-ordinate-method radiative transfer in scattering and emitting layered media, *Appl. Opt., 27*, 2502, 1988.

Stasiewicz, K., On the origin of the auroral inverted-V electron spectra, *Planet. Space Sci., 32*, 379, 1984.

Störmer, C., *The Polar Aurora*, Clarendon, Oxford, 1955.

Strickland, D. J., D. L. Book, T. P. Coffey, and J. A. Fedder, Transport equation techniques for the deposition of auroral electrons, *J. Geophys. Res., 81*, 2755, 1976.

Swartz, W. E., J. S. Nisbet, and A. E. S. Green, Analytic expression for the energy-transfer rate from photoelectrons to thermal electrons, *J. Geophys. Res., 76*, 8425, 1971.

Walker, J. C. G., and M. H. Rees, Ionospheric electron densities and temperatures in aurora, *Planet. Space Sci., 16*, 459, 1968.

Winningham, J. D., T. W. Speiser, E. W. Hones, Jr., R. A. Jeffries, W. H. Roach, D. S. Evans, and H. C. Stenbaek-Nielsen, Rocket-borne measurements of the dayside cleft plasma: The tordo experiments, *J. Geophys. Res., 82*, 1876, 1977.

Winningham, J. D., D. T. Decker, J. U. Kozyra, J. R. Jasperse, and A. F. Nagy, Energetic (> 60 eV) atmospheric photoelectrons, *J. Geophys. Res., 94*, 15,335, 1989.

D. Lummerzheim, Q.-L. Min, M. H. Rees, and K. Stamnes, Geophysical Institute, University of Alaska, Fairbanks, AK 99775-0800.

(Received October 19, 1992;
revised May 17, 1993;
accepted June 14, 1993.)